Level-1 Trigger Algorithms at CMS for the HL-LHC

Jack Li
Northeastern University
on behalf of the CMS Collaboration
ICHEP, 28 Jul-6 Aug, 2020

Introduction

The CMS experiment is planning to upgrade its trigger system in the light of HL-LHC. The L1 trigger will benefit from the addition of tracking information as well as the updates of subdetectors. A panel of L1 trigger algorithms are presented targeting physics objects including:

- Electrons and photons.
- Jets.
- Tau leptons.
- Energy sums.

While more complex algorithms that take information from the full detector or multiple subdetectors have delivered a robust performance, algorithms that only take subdetector information have also demonstrated their comparable trigger efficiency on simulated L1 objects and resilience to pileup.

The expected performance of these algorithms are evaluated based on simulated samples produced choosing a center of mass energy of **14 TeV** and an average of **200** collisions per bunch crossing.

Figure 2: ROC curve of the BDT classifier for e/γ objects in the endcap calorimeter.

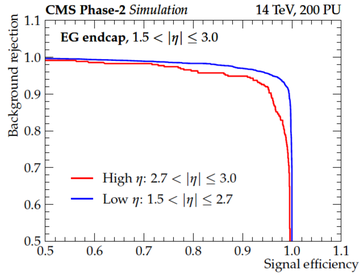

Figure 3: $\Delta\eta$ vs $\Delta\phi$ distances between calorimeter clusters and the closest L1 track.

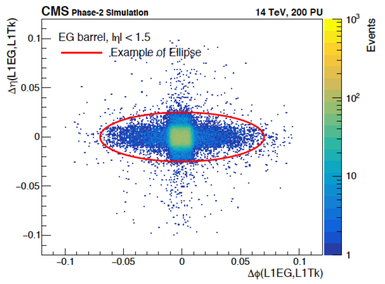

LVX VERITAS VIRTVS
Northeastern University

Electrons and Photons

In phase II, the reconstruction of e/γ candidates will benefit significantly from the improved granularity in barrel calorimeter, where the highest-p_T trigger primitive with $p_T > 1$ GeV is chosen as the seed. Areas of different sizes near the seed crystal are used for different purpose [Fig. 1].

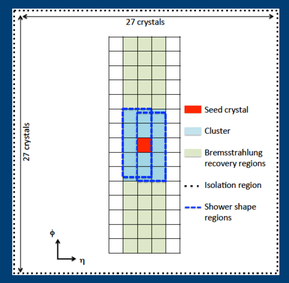

Figure 1: The geometry of the e/γ clusters in the barrel.

The ECAL endcap will be replaced with HGCAL, which provides detailed 3-dimensional shower information. To exploit the full potential of this information, a BDT [Fig. 2] is implemented to distinguish signal candidates from clusters originated from pileup.

The addition of tracking information provides another powerful handle to keep the physics objects resilient to pileup. Centered on each cluster, an elliptical cut in the $\eta - \phi$ plane [Fig. 3] is defined as

$$(\Delta\eta/\Delta\eta_{\max})^2 + (\Delta\phi/\Delta\phi_{\max})^2 < 1. \quad (1)$$

Clusters with at least one matched track are promoted to track-matched electron candidates. While losing some efficiency in both barrel [Table 1] and endcap driven by the track reconstruction, the track-matched algorithm reduces the trigger rate [Table 2] to an even lower level.

Efficiency	calorimeter only	track-matched
30GeV	97.5%	84.5%
40GeV	98.7%	88.0%

Table 1: Single electron efficiency in the barrel calorimeter.

Rate	calorimeter only	track-matched
30GeV	78.2 kHz	19.0 kHz
40GeV	25.5 kHz	8.3 kHz

Table 2: Trigger rate of the barrel L1 objects.

Jets

- Calorimeter based:

This algorithm forms jets from tower information provided by calorimeter. A 7×7 configuration is chosen as the jet size. The jet is corrected for energy reconstruction and PU. The trigger turn-on curve for this algorithm has a steep rising edge at the threshold value while the efficiency is almost flat across the full η spectrum.

- Track based:

Tracks satisfying the purity requirement in [Table 3] are clustered by this jet finding algorithm using a nearest-neighboring approach. It has been shown that the performance of this L1 track-based clustering is similar to that of a full anti-k_T clustering with FASTJET. A firmware implementation is available and has been tested in a hardware demonstrator.

Track Variable	Cut
N_{stubs}	≥4
p_T	≥2GeV
χ^2/dof	<40
χ^2_{bend}	<2.4

Table 3: L1 track purity requirement.

- Particle-flow based:

The PUPPI candidates are binned by PF-based algorithm into pseudo trigger towers. A 7×7 window centered on a local maximum is defined [Fig. 4] to build jets. Jet energy correction factors are applied based on the jet momentum and position. It has been shown that this algorithm has an improved jet response and energy resolution when compared to calo-only or track-only jet finding. Both the efficiency [Fig. 5] and the rate produced by this algorithm is close to that of the offline AK4 algorithm when using PUPPI inputs. This algorithm has been implemented in HLS and tested in a hardware demonstrator. It is estimated that the resources usage of this algorithm is within the availability.

Figure 4: The geometry of PF-based jet finding.

A comparison of these jet finding algorithms is shown in [Fig. 6].

Tau Leptons

- Calorimeter based:

While a different jet size (3×5) [Fig. 7] is chosen, the calo-based τ reconstruction algorithm in the barrel is very similar to the calo-based jet finding algorithm. Further optimization is possible in HGCAL with the implementation of BDT.

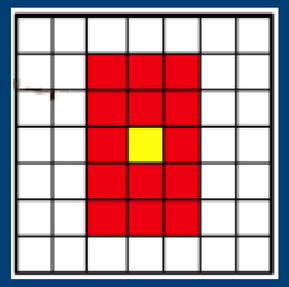

Figure 7: The geometry of Calo-based τ reconstruction.

- Track+e/γ:

Track+e/γ algorithm builds up τ candidates by associating e/γ clusters to the track-only objects. It is has been shown that this algorithm delivers very good efficiency that is comparable to other complex algorithms.

- Particle-flow based:

The PF-based approach takes either PUPPI or PF candidates and utilizes a dense neural network to help identify τ candidates. A cut is placed on the neural network output to reduce the rate for lower-p_T particles. It has been shown that the addition of jets in the final state selection helps to improve the τ reconstruction efficiency from 89% to 94% in the barrel. It is estimated that this algorithm is capable of identifying a τ every 25 ns with an improved efficiency despite the complicated firmware.

A comparison of these algorithms is shown in [Fig. 8].

Energy Sums

- Track based:

Track purity requirement [Table 3] is applied to minimize of the impact of bad-seeded tracks in the calculation of MET. The performance of this algorithm is gauged by applying the algorithm to simulated tracking particles. It has been shown that applying the full track selection reduces the trigger threshold from 200 GeV to 70 GeV.

- Particle-flow based:

The PF-based algorithm applies PUPPI algorithm to PF candidates to before the calculation of E_T^{miss}. The threshold cluster p_T in HF is optimized to minimize pileup contribution. It is estimated using HLS that there are less than 90 PF candidates in 95% of events after PUPPI to be included in the E_T^{miss} calculation. The performance of this algorithm has been evaluated for both $t\bar{t}$ and VBF process. It has been shown that this algorithm produces a sharper trigger turn-on when compared to track-only E_T^{miss} reconstruction.

A comparison of these algorithms is shown in [Fig. 9].

Figure 5: Single jet trigger efficiencies in QCD and $t\bar{t}$, for 9×9 histogramed jets and AK4 jets, using PUPPI inputs.

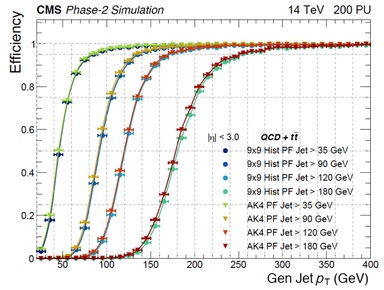

Figure 6: Comparison of the performance of different jet finding algorithms in $t\bar{t}$ events.

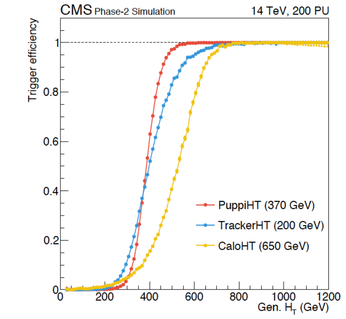

Figure 8: Single τ trigger efficiency for different τ_h reconstruction algorithms.

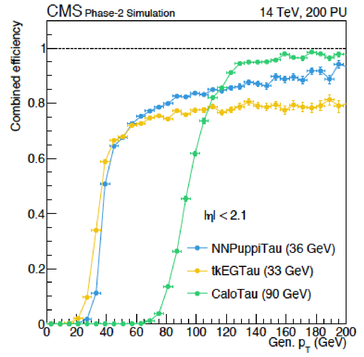

Figure 9: The combined matching and turn-on trigger efficiency for different missing transverse energy algorithms.

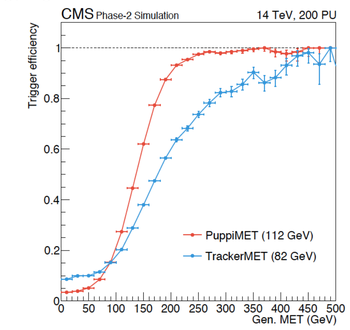

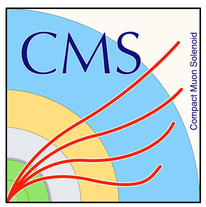

Reference

CERN-LHCC-2020-004

CMS-TDR-021